Colloid and Polymer Science (2018) 296:1173–1182
https://doi.org/10.1007/s00396-018-4328-5

ORIGINAL CONTRIBUTION

Facile protein-resistant and anti-biofilm surface coating based on catechol-conjugated poly(N-vinylpyrrolidone)

Ai-Nhan Au-Duong[1] · Cheng-Kang Lee[1]

Received: 2 March 2017 / Revised: 27 March 2018 / Accepted: 26 April 2018 / Published online: 22 May 2018

Abstract

A facile biofouling-resistant surface coating was developed based on catechol-conjugated poly(N-vinylpyrrolidone) (CA-PVP). CA-PVP can be securely and effectively coated on glass, gold, and tissue culture polystyrene (TCPS) surfaces under a mild condition as characterized by ATR-FTIR and PVP-complexation with iodine and hydrogen peroxide. PVP itself without catechol conjugation, on the other hand, cannot achieve well-coating on surfaces. The coated surfaces became more hydrophilic and protein-resistant due to the presence of PVP as measured by the reduced contact angles and surface plasmon resonance (SPR) responses. The significantly enhanced protein resistance created by CA-PVP coatings leads to its significant anti-biofilm and fibroblast cell adhesion resistance as observed by fluorescent microscope. CA-PVP coating also demonstrated its high biocompatibility that ≥ 95% cell viability of mouse fibroblast cells still can be maintained after 48 h cultivation.

Keywords Anti-fouling · Catecholic poly(N-vinylpyrrolidone) · Crosslinked PVP · Biomacromolecule adhesion · High effect

Introduction

In recent time, implantations of biomaterials and/or medical settings in human body have become more routinely performed to improve the life quality of patients. However, the performance of implanted biomaterials usually will be hampered by the nonspecific deposition of proteins from the body fluid soon after implantation. The deposition of proteins on the surface of in vivo biomedical devices can also promote attachment of bacteria to form a biofilm which can cause serious health-associated infections. According to the report of National Institutes of Health, 75% of human microbial infections are caused by bacterial biofilm [1]. Biofilm is very difficult to treat with antibiotics due to the fact that bacteria are well-encapsulated in a robust biofilm matrix, consisted of high density of surface-attached proteins, exopolysaccharides, and extracellular DNA (eDNA) [1, 2]. Therefore, an effective way to prevent bacteria from surface attachment to form biofilm is to overcome the nonspecific adsorption of proteins on the surface. An anti-fouling (AF) coating that makes the surface inert to processes in the human body is highly desirable. A variety of chemically polymerized surfaces with hydrophilic polymers such as poly(ethylene glycol), poly(methyl methacrylate-*co*-butyl acrylate), and polymers containing zwitterion functionalities are widely used as anti-fouling coatings due to their very low-protein adsorption property [3–7]. In addition to anti-fouling coating for the prevention of nonspecific protein surface adsorption, anti-biofilm coatings have also been developed to incorporate antimicrobial agents, for example, quaternary ammonium compounds and silver nanoparticles which possess stronger antimicrobial titer with the polymeric coating materials to kill the bacteria for the prevention of biofilm formation [8, 9]. In contrast to the anti-fouling coatings, the antimicrobial compounds involved anti-biofilm coating may have to face with more environmental considerations and the increased costs in preparation [10].

Poly(N-vinylpyrrolidone) (PVP) is a well-known nontoxic, water-soluble, bioinert, and chemically stable polymer with resistance against a wide range of biofouling compounds [11–13]. PVP as anti-fouling coatings are often prepared by grafting PVP from a substrate surface, using surface-initiated atom transfer radical polymerization (ATRP) of N-vinylpyrrolidone (NPV) [11–15]. The ATRP method for

Electronic supplementary material The online version of this article (https://doi.org/10.1007/s00396-018-4328-5) contains supplementary material, which is available to authorized users.

✉ Cheng-Kang Lee
cklee@mail.ntust.edu.tw

[1] Department of Chemical Engineering, National Taiwan University of Science and Technology, 43 Keelung Rd. Sec. 4, Taipei, Taiwan 106

grafting PVP on surface, although quite effective for preventing nonspecific protein adsorption, requires complicated chemical synthetic steps for immobilizing initiator on the surface as well as for the preparation of catalytic agents. Simpler methods but require special equipment such as UV-induced photo grafting [16], γ-radiation-induced grafting [17, 18], and plasma polymerization [19] have also been developed to modify the surface of polymeric membranes with hydrophilic PVP. Anti-fouling PVP coatings were also often prepared by cross-linking into hydrogel to make the polymer insoluble when in contact with body fluid. Electron beam [20], redox reactions [21], or UV-activated molecules [16] have been used as cross-linking agents of PVP coating. In addition, generation of radicals in PVP for cross-linking by thermal annealing has been proposed [22]. Telford et al. not only characterized the thermal annealing cross-linked PVP films but also demonstrated their excellent protein-repellent properties [23]. However, a minimum of 200 °C for 3 h is required for the thermal annealing cross-linking which may damage the supporting substrate. Recently, a facile and versatile aqueous surface modification technique based on mussel-inspired surface chemistry using dopamine as a modifier has been developed by Messersmith et al. and widely employed for coating on various materials [24, 25]. Dopamine is able to undergo self-polymerization in aqueous solution under oxidative conditions, creating an adherent polydopamine (PDA) adlayer onto various substrate surfaces. Anti-fouling PVP coating can be easily formed on the PDA-coated surface via hydrogen bonding interactions [26]. Nevertheless, the major challenges in this method, including possible loss of PVP coating from PDA adlayer and easy loss of PDA adlayer from flat substrate surface due to the noncovalent bonding interactions, and significant loss of transparency of substrate due to the dark color of PDA.

The key aspect of mussel-inspired surface chemistry is the ortho-dihydroxyphenyl (catechol) functional groups in mussel adhesive protein structure which forms strong bonds with various surfaces [27–29]. Inspired by these facts, various polymers bearing catechol side chains have been designed and synthesized to achieve facile coating of polymers on various substrate surfaces for biomedical application [30–35]. Recently, copolymers of PVP backbone with catechol side chains have been synthesized for the preparation of robust underwater biomimetic adhesives [36]. A much simpler one-step conjugation method for grafting catechol groups to PVP (CA-PVP) has also been developed by Mosaiab et al. for covalent attachment of PVP onto the magnetic core that can facilitate silver nanoparticle formation for antibacterial treatment [37]. However, this CA-PVP surface coating against biofouling has never been reported. In this work, we take the advantage of CA-PVP on its easy preparation for facile surface modification of PVP onto several substrate surfaces. The aim of the present work is to study the effect of this facile one-step coating on fouling resistant against proteins, bacterial biofilm, and mammalian cells. The anti-biofouling activity of PVP-grafted substrates was evaluated with their performances against the bovine serum albumin protein, L929 cell, and Gram-positive *Staphylococcus epidermidis* bacteria. The biocompatibility of PVP-immobilized surface was also studied.

Materials

Poly(N-vinylpyrrolidone) (PVP, MW = 10,000), bovine serum albumin (BSA), and fluorescein isothiocyanate (FITC) were purchased from Sigma–Aldrich. 2-Chloro-3,4′-hydroxyacetophenone (97% ACS) was obtained from Alfa Aesar. All other chemicals were reagent grade.

Synthesis of catechol-grafted poly(N-vinylpyrrolidone)

2-Chloro-3,4′-hydroxyacetophenone (CA) was employed to conjugate catechol groups to the structure of polyvinylpyrrolidone (PVP) based on the method described elsewhere [37]. Briefly, CA and PVP with mole ratio of 30:1 were dissolved in 25 ml of ethanol in a reagent tube. After purging with nitrogen gas for 30 min, the reaction was then carried out at 70–80 °C under magnetic stirring for 24 h. After reaction, the solution was concentrated in a rotary evaporator, and ample amount of cold diethyl ether was then added to induce the precipitation. After washing thoroughly with diethyl ether, the obtained precipitate was dried in a vacuum oven and used as CA-PVP.

PVP coating

Typically, the substrates including glass slide disc with a size of 1-cm diameter were first immersed in coating solutions prepared by dissolving 50 mg CA-PVP or PVP in the mixture of ethanol (5 mL) and deionized water (3.75 mL). Tris buffer (pH 8.5) of 2.5 mL was then added to the above mixture. The solution immediately turned into pale yellowish and gradually changed to brownish. The reaction was allowed to proceed for 12 h. Later, 10 mM $NaIO_4$ of 12 μL was added, and the reaction continued for another 12 h. The substrate was then taken out from the reaction solution and rinsed thoroughly with deionized water followed by ethanol.

Protein adsorption

Bovine serum albumin (BSA) was first fluorescent-labeled with fluorescein isothiocyanate (FITC) as described elsewhere [38]. The labeled BSA was diluted with 1× PBS buffer (pH = 7.4) to a concentration of 1 mg/mL. The bare glass and CA-PVP-coated glass surfaces were pre-wetted in pH 7.4 PBS

before incubation in the labeled BSA solution at room temperature for 24 h. After incubation, the glass surface was rinsed three times (10 min each) with PBS and observed by confocal laser scanning microscopy (CLSM, Olympus IX73). For evaluating the protein-binding resistance toward the CA-PVP-coated surface, BSA protein solution of 1 mg/mL was employed to interact with CA-PVP-coated gold surface of the sensor chip in surface Plasmon resonance (SPR) study using Autolab SPRINGLE instrument. This instrument uses a photodiode detector (p-polarized, $\lambda = 670$ nm) to record the SPR angle shift from light-reflecting at the interface (1 mm × 2 mm spot of the sensor disk). The incidence angle can be varied an angle of 5° in approximately 13 ms by using a scanning mirror with a frequency of 76 Hz.

Biofilm formation

Staphylococcus epidermidis (ATCC 35984) was cultured in TSB nutrient medium overnight. Then, 1 mL of bacterial suspension with the cell concentration of 10^6 cells/mL was added to each bare or coated well in a PS 24-well plate (Jet Biofil®). Biofilm formation on glass surface was also studied by culturing 1 mL bacterial suspension in the wells containing glass slide with coated surface faces the bacterial solution in a 24-well plate. The bacterial cells were allowed to grow at 37 °C for 72 h in static. After decanting the solution in the wells, the fresh culture medium was replenished, and the cultivation was continued for another 24 h. The surfaces of substrates were washed thoroughly with PBS prior to further biofilm quantitative analysis and fluorescence imaging observation.

For quantitative analysis of biofilm on the surface, crystal violet staining was employed. Methanol of 1 mL was filled to each well and incubated for 20 min. The methanol solution was then removed, and the wells were air-dried for 5 min before filling with 1 mL of 0.1% (*w*/*v*) crystal violet to stain the biofilm for 15 min. After the crystal violet solution of each well was removed, DI water was added to wash the well for three times. The washed well was air-dried before 1.5 mL 33% acetic acid was added to extract dark blue color stained on the biofilm. Finally, the optical density of each well was measured at 570 nm (OD_{570}) in order to quantify the amount of formed biofilm on the surface.

BacLight LIVE/DEAD Bacterial Viability Kits (Life Technologies, Catalog number L7012) was also employed to verify the live and dead bacterial cells on the surface. In detail, each 1.5 μL of SYTO9 dye (component A) and propidium iodide (component B) was mixed together with 1 mL 1× PBS, and the mixture were placed on the glass surface for dying 15 min. Fluorescence images on the dyed surface were observed by fluorescence microscope (Olympus IX73).

Cell adhesion

L929 mouse fibroblasts cells were first grown in DMEM nutrient medium. The 1-mL cell solution at a density of 10^4 cell/mL was then seeded into the 24-wells plate containing glass slide on the bottom of the well. After cultivation at 37 °C for 24 h in static, the glass slide surface was washed with PBS 1× for three times. The number of cell attachment on the glass surface was quantitatively measured by colorimetric LDH assay. LDH analysis solution was prepared by mixing solutions (in PBS 1× at pH 7.4) of 4 mg/mL INT dye, 36 mg/mL sodium lactic acid, 12 mg/mL NAD, 1.2 mg/mL BSA, 48 mg/mL Sucrose, 5.4 mg/mL *Diaphorase* with volume ratio of 4:4:1:1:1:1. For evaluation, 0.5 ml of 0.1% Triton was added and shaken at 100 rpm for 30 min to lysis the cell membrane. Fifty microliters of supernatant was incubated with 60 μL reaction mixture at 37 °C for 30 min, the optical density at 490 nm was valued.

Biocompatibility

To test the cytotoxicity of coating surface, the 1 cm × 1 cm coating samples were immersed in 1 mL DMEM medium for 1, 3, and 5 days at 37 °C to extract the releasable chemicals from the coating. L929 cells were pre-culture into 96-well plates for 24 h at a density of 10,000 cells/well. After incubation at 37 °C under 5% CO_2 atmosphere, 100-μL cell suspension in each well was replaced with the extracted solutions. After 24 and 48 h of incubation, the viability of cells in plates was measured by MTT assay. MTT solution (5 mg/mL in PBS 1×) of 20 μL/well was added to each well and incubated for 4 h at 37 °C in a 5% CO_2 humidified atmosphere. The solution in each well was then removed and refilled with 200 μL/well DMSO to dissolve the formed formazan crystals. The optical density (OD) of DMSO solution in each well was recorded at 570 nm.

Characterization

Scanning electronic microscope (SEM) (JEOL, Japan, JSM-6500F) operated at 15 kV was used for surface observation. Attenuated total reflection–Fourier transform infrared spectrophotometer (FTS-3500, Bio-Rad) was employed for analyzing the chemical structure of the coating surface. The optical density (OD) values of the samples were measured by Biochrom® Asys UVM340. The transmittance of PVP and CA-PVP-coated glass surface was recorded with Jasco V-730 UV-Vis spectrometer. The wettability of the substrates was evaluated by measuring the static contact angles (Sindatek) with deionized water (10 μL droplet volume). The value was recorded at least five replicates for each sample.

Results and discussion

Preparation and characterization of CA-PVP-coated surface

Catechol-conjugated poly(N-vinylpyrolidone) (CA-PVP) was synthesized by quanternizing the amino group in the pyrrolidone structure of PVP by using 2-chloro-3,4′-hydroxyacetophenone following the same procedure reported by Mosaiab et al. [37]. Structural analyses of the as-prepared CA-PVP were confirmed by the ^{1}H-NMR and FT-IR spectroscopy. As shown in the Fig. S1, ^{1}H-NMR spectra of the synthesized CA-PVP conjugation in D_2O were found to have not only very strong peaks of PVP polymer in the range of 1.0–4.0 ppm, which correspond to 1.00–2.60 ppm for six protons per unit of lactam CH_2 and backbone CH_2; 3.0–4.0 ppm for three proton per unit of lactam CH_2 (linked to amide group) and backbone CH, but also additional signals at 7.0–7.6 ppm indicating for the presence of catechol protons. This suggests successful quanternized grafting catechol groups to PVP. The catechol content of the as-prepared CA-PVP was determined to be 22 catechols per PVP chain based on the integrated value difference of the proton 2.2–2.6 ppm of NVP unit (four protons) and the proton 7.0–7.12 ppm of catechol (one proton). Moreover, glass slide surface was drop-coated with CA-PVP and characterized by ART-FTIR. As shown in Fig. 1a and S2, very strong absorption bands observed at 1170 and 810 cm^{-1} for every sample resulted from the Si–O–Si asymmetric/symmetric stretch of glass material. In comparison with bare glass surface, several weak absorption peaks at 2959, 1420, and 1280 cm^{-1} corresponding to the stretching vibration of methylene group (–CH_2–) and (–CH–) bend appeared in PVP and CA-PVP-coated sample surface. Remarkably, carbonyl group (C=O) in the pyrrolidone ring vibration at 1770 cm^{-1}, amide linkage (O=C–NH–), C–N bend at 1660 cm^{-1} or (N–C=O) bend at 690 and 590 cm^{-1} in CA-PVP were slightly shifted in comparison with unmodified PVP. These indicate not only the synthesis of CA-PVP but also the CA-PVP coating were successfully obtained. Approximately, 65 ± 10 μg/cm^2 of CA-PVP was coated on a glass slide as estimated by measuring the weight gain after drop-coating. In the UV-Vis spectrum of CA-PVP (Fig. 1b), absorbance peaks for the catechol group and PVP polymer were found at 280 and 210 nm which is again confirmed the successful conjugation of CA to the structure of PVP polymer. Besides, diffuse reflectance UV-Vis spectra could more clearly characterize the optical properties of the surface-coated CA-PVP as shown in Fig. S3. The CA-PVP coating did not affect the absorbance of glass slide much; however, a peak at 220 nm in CA-PVP coating was noted which is slightly left-shifted from the peak of bare glass but close to the peak of PVP itself.

Due to their preference of forming complex with PVP, H_2O_2 and I_2 were loaded on the coated surface, and their presence was detected to show the success of facile coating of PVP on glass surface via catechol groups of CA-PVP was achieved. The presence of H_2O_2 was checked by its ability to reduce $KMnO_4$ that leads to the disappearance of purple color of $KMnO_4$. The presence of iodine was demonstrated by the purple color developed due to the complex reaction between starch indicators and iodine. After loading the H_2O_2 on surface, as shown in Fig. 2c, light purple color of $KMnO_4$ remained on the bare glass and PVP coated surface. In contrast, the purple color of $KMnO_4$ faded away immediately on CA-PVP coating surface. Similarly, a weak but apparent color change was observed when iodine-loaded CA-PVP coating was incubated in 1% starch indicator solution. The iodine

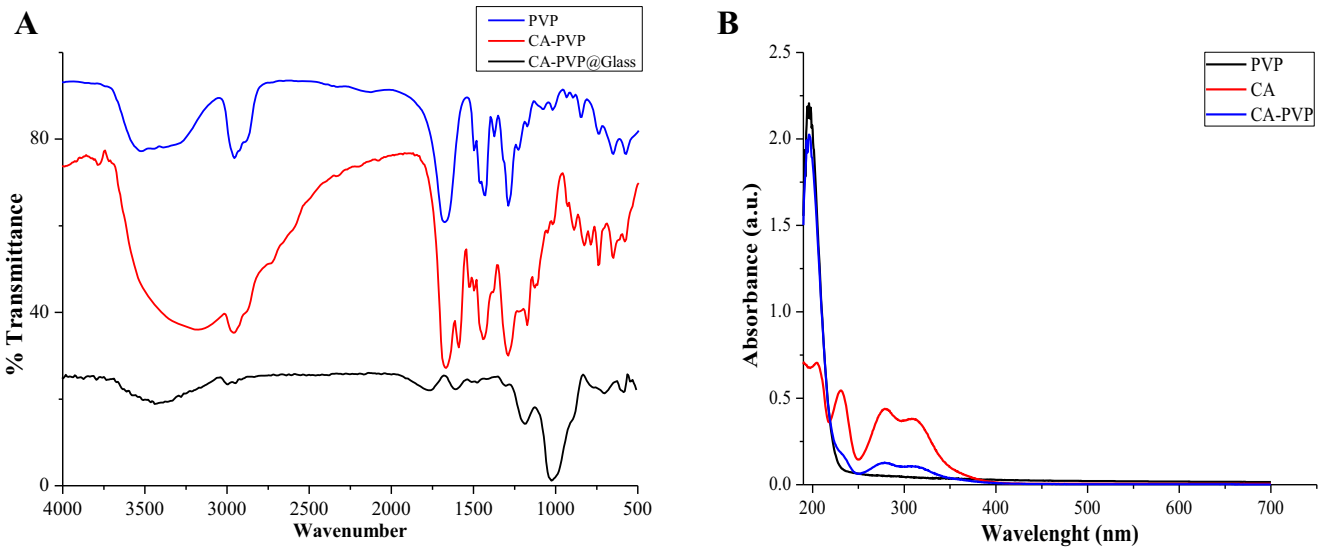

Fig. 1 (**a**) FT-IR spectra of PVP, CA-PVP, and CA-PVP drop-coated glass and (**b**) UV-Vis spectra of PVP, CA, and CA-PVP prepared in DI-water at concentration of 10 μg/ml

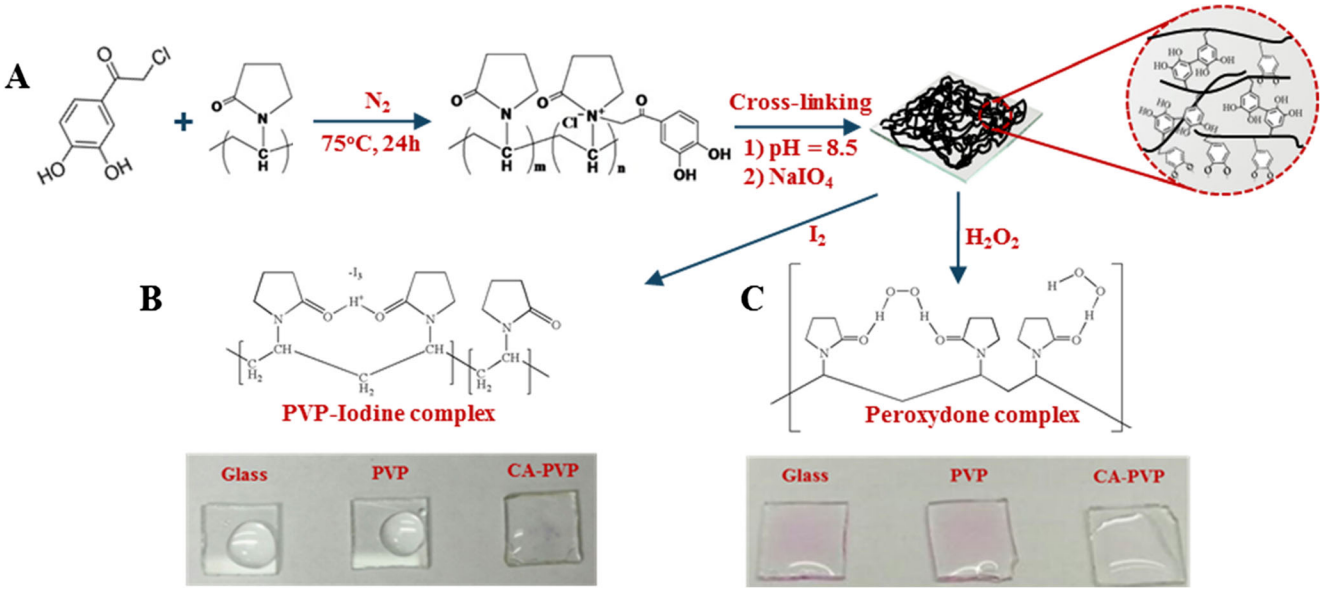

Fig. 2 (**a**) Schematic illustration of functionalization of polyvinylpyrrolidone with catechol groups (CA-PVP preparation) and its surface coating via oxidative cross-linking. Colorimetric assay of the presence of PVP- on CA-PVP-coated surface, (**b**) iodine-complexed surface generated slightly blue-color when a droplet of starch indicator solution (1%) was applied, (**c**) H_2O_2 complexed surface discolored the purple color of applied $KMnO_4$ solution

complexes with CA-PVP coating also demonstrated its antimicrobial activity against *E. coli* as shown by a clear zone formation around the sample disc in the inhibition zone test. In contrast, no appreciable clear zone could be observed for the bare glass and PVP coating samples (Fig. S4). Evidently, only CA-PVP coating can make PVP persists on glass surface after thoroughly washing with water. The oxidative catechol groups of CA-PVP play the major role for PVP adhering on the glass surface.

The wettability of PVP- and CA-PVP-coated surfaces was also compared to demonstrate the effect of CA conjugation on improving the adhesion of PVP onto the surface. As shown in Fig. 3, contact angles of water droplet on bare glass, gold, and PS surface were 30°, 78°, and 89°, respectively. After PVP coating and thoroughly washing, the contact angles of glass and PS surface decreased slightly to 28° and 73°, respectively. In contrast, the contact angle reduction on gold surface was quite significant to 55° that indicates some of the hydrophilic PVP molecules persist on the surface after thoroughly rinsing with water. The strong interaction of PVP toward noble metallic surface has been known previously and frequently employed as a steric stabilizer or capping agent for the noble metal nanoparticles [39]. When CA-PVP coatings were applied on the surfaces of these materials, the contact angles were significantly decreased to 8°, 18°, and 54° for glass, gold, and PS surface, respectively. Evidently, CA-PVP was much effective to be coated on these surfaces in comparison with PVP, and the originally more hydrophilic surface, such as glass surface was much easier to be coated with CA-PVP to generate a nearly super hydrophilic surface.

Anti-fouling property

Protein adsorption

Bovine serum albumin (BSA) was used as model protein to investigate the effect of CA-PVP coating against protein adsorption. Surface plasmon resonance (SPR) analysis employed to study the real-time BSA adsorption behavior on CA-PVP-coated gold surface of a SPR sensor chip. In SPR measurement, BSA solution was loaded into a solution

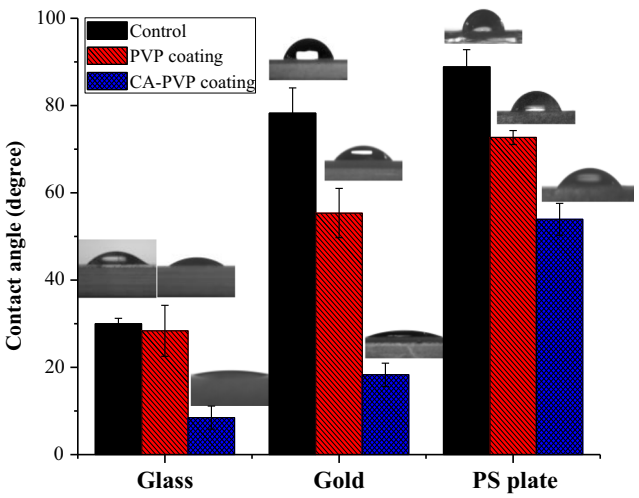

Fig. 3 Contact angle images and value of bare-, PVP-, and CA-PVP-coated surfaces (glass, gold, and PS). All the surfaces were under the same pre-treatment for drying before H_2O was employed for contact angles measurement

that continuously pumped over the SPR sensor surface, and bound BSA mass was followed as response units (RUs) in a sensogram, which shows the RU as a function of time. SPR sensor chips of bare and PVP-coated surfaces were used as a negative and positive control, respectively. As demonstrated in Fig. 4, a significant increase of RU was observed on bare surface in comparison with PVP- and CA-PVP-coated surfaces when BSA was injected. When estimated by RU difference from the base line, only about 50% of BSA bound onto the surface during the loading period was eluted from bare gold surface. In contrast, approximately 75 and 90% of adsorbed BSA were washed away from PVP- and CA-PVP-coated gold surface, respectively. Apparently, the effectiveness of protein adsorption resistance of PVP and CA-PVP coating is much better than that of bare gold surface. Out of our expectation, PVP coating also shows good performance on protein adsorption resistance although its effectiveness is still inferior to that of CA-PVP coating. This indicates that PVP itself has a strong interaction toward gold surface in comparison with glass surface. The similar results were also observed on wettability study shown in Fig. 3 that PVP itself has a stronger adhesion on gold surface rather on glass surface. In other words, once drop-coated on gold surface, PVP cannot be completely displaced by water molecule. The protein-binding resistance of different coating surfaces was also studied by employing fluorescent FITC-BSA as a model protein. As shown in Fig. 5 and S5, very bright fluorescence was observed on bare and PVP-coated surface by fluorescence microscope after incubating FITC-BSA on the surfaces followed by thoroughly washing. In contrast, no trace fluorescence could be observed on the CA-PVP-coated surface under the same conditions. Evidently, CA-PVP is much effective to be coated on glass surface than PVP to prevent protein from binding onto the surface. This result again confirms what observed in previous section that H_2O_2 and iodine could only be detected on the CA-PVP-coated glass surface due to their complex interaction with immobilized PVP.

Anti-biofilm and cell adhesion

S. epidermidis is well-known for its biofilm formation capacity that most often causes biomaterial-associated infections [40]. Therefore, *S. epidermidis* was employed to test the anti-biofilm capacity of PVP- and CA-PVP-coated surfaces. The bacterial cells were cultured in a 24-well plate with coated bottom surface or containing surface coated glass discs of 1 cm in diameter. The amount of biofilm formed on the surface was quantified by crystal violate staining. As shown in Fig. 6a, the bare surfaces have the deepest purple color which reflects a thick biofilm was formed. When PVP was coated, the amount of biofilm formed on the surfaces reduced. But, the amount on PS surface was much higher than that on the glass surface. Based on the color intensity of acetic acid extraction solution (33%) of the stained surface (Fig. 6b), the amount of biofilm on PVP-coated PS surface was estimated to be approximately fivefold higher than that on coated glass surface. Since proteins bound to the surface is the initial step for the biofilm development, the much higher amount of

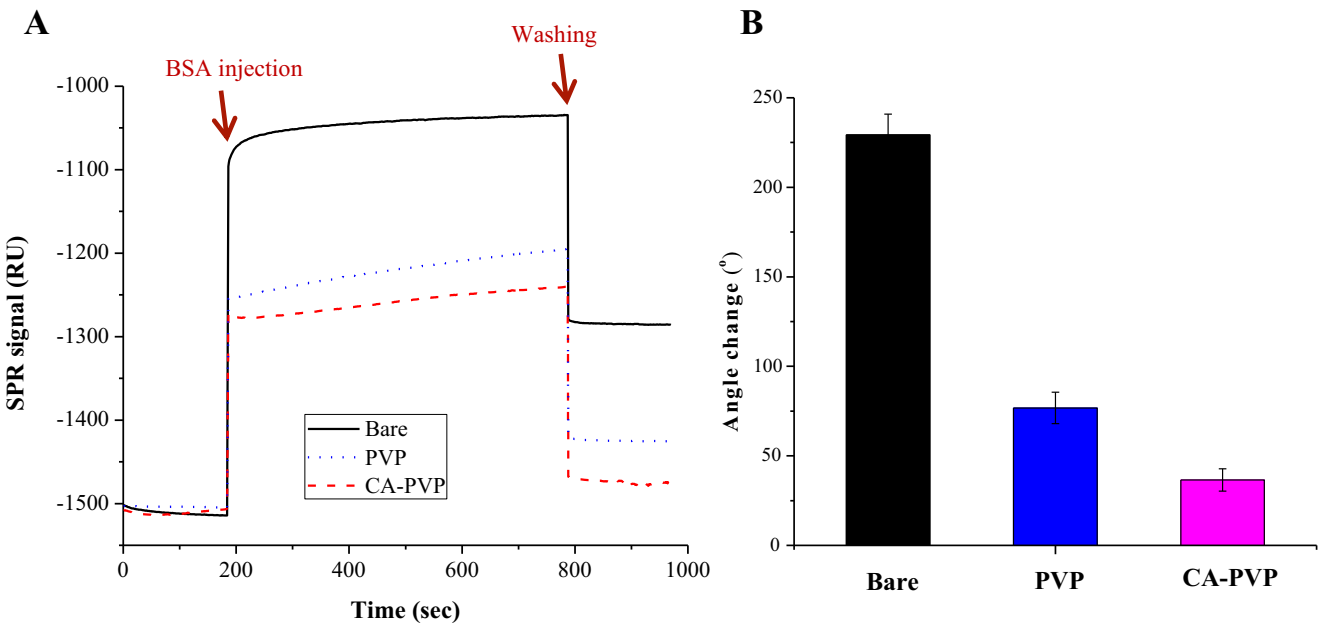

Fig. 4 (**a**) Real-time response of protein adsorption on bare-, PVP-, and CA-PVP-coated gold chip surfaces of surface plasmon resonance (SPR) sensors at room temperature and BSA protein solution of 1 mg/mL. (**b**) Increases of SPR signal units after BSA adsorption followed by buffer washing

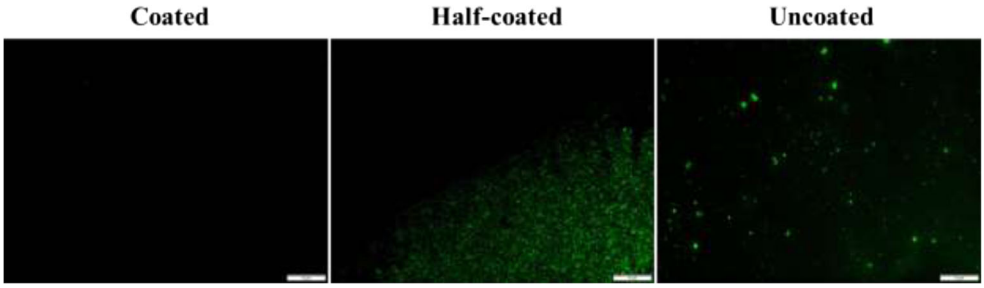

Fig. 5 Fluorescence images of green-color FITC-BSA protein adsorption on CA-PVP-bare (control), CA-PVP-coated, and CA-PVP-half-coated surface resulted by contacting labeled protein solution of 1 mg/mL at room temperature

biofilm observed on PVP-coated PS surface can attribute to its lower wettability (higher hydrophobicity) (Fig. 3) which generally leads to an enhanced protein adsorption as shown by the stronger fluorescence intensity observed from FITC-

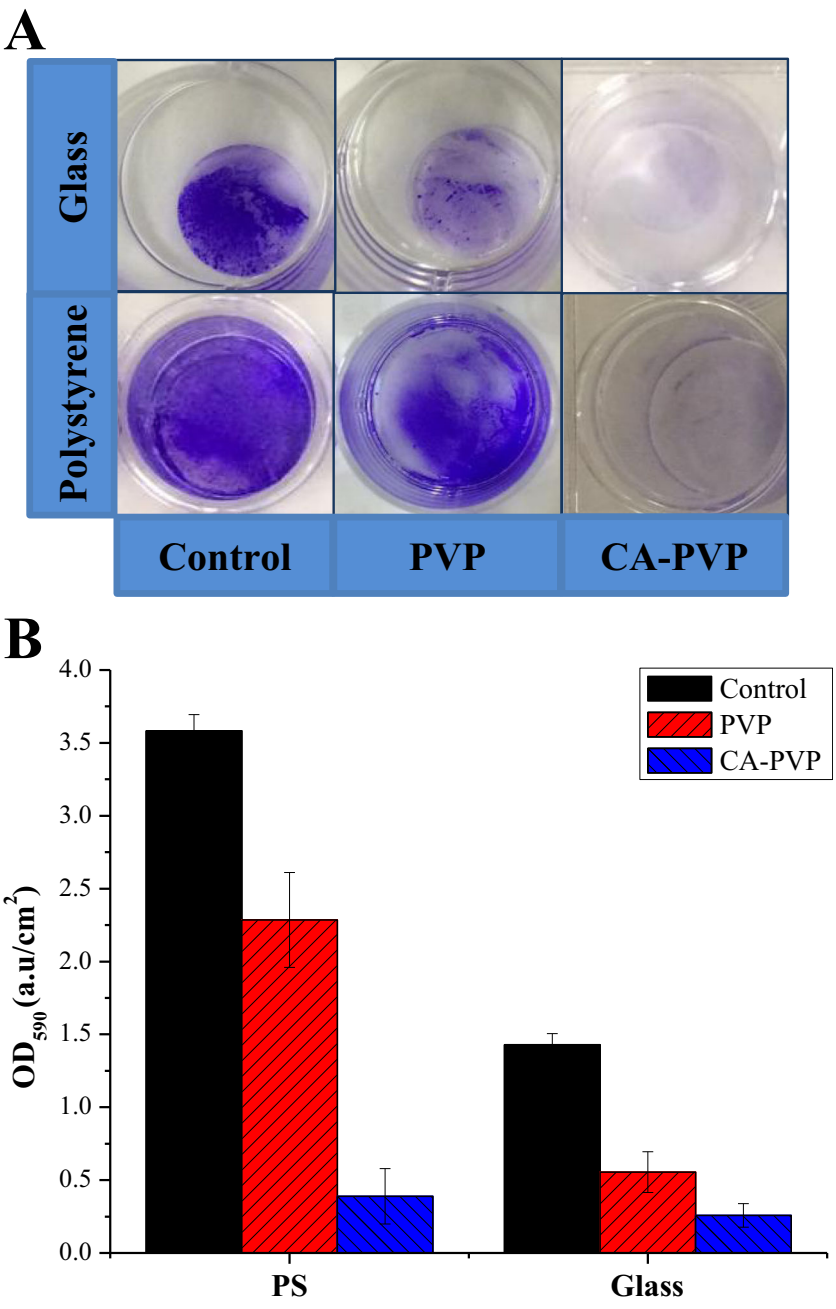

Fig. 6 Observation of *S. epidermidis* biofilm formed on glass and polystyrene substrate at 37 °C by (**a**) photo image of crystal violet-stained biofilms and (**b**) OD_{590} of the destained solutions

BSA surface binding (Fig. 5). In contrast to PVP coating, CA-PVP-coated surfaces either on PS or glass shows no appreciable biofilm formation (Fig. S6). The biofilms on different coating surfaces were also observed by fluorescent microscope after Baclight LIVE/DEAD staining. As shown in Fig. S6, the number of cells on bare glass surface is much higher than that of PVP- and CA-PVP-coated glass surface. Barely, bacterial cells can be observed on CA-PVP-coated surface. These results show that CA-PVP coating was not only generating a protein-resistant surface but also a very effective anti-biofilm surface.

The effect of PVP coating on the surface adhesion of mouse fibroblast L929 cells was also studied. As observed by Fig. 7, the amount of cells adheres to the surfaces follows the similar trend as the amount of biofilm formed on the coating surfaces. Bare surface has the highest amount of L929 cells while very few cells could be observed on CA-PVP-coated surface. Evidently, the presence of PVP on the CA-PVP coating surface is not favorable for the fibroblast cells to anchor and grow because of its anchorage-dependent growth nature. On the other hand, PVP without conjugated with CA cannot be well-coated on glass and TCPS surface, as a consequence, an appreciable amount of L929 cells still can adhere and grow on PVP-coated surfaces. The cytotoxic effect of CA-PVP coating was also studied by culturing L929 cells in CA-PVP coating extract prepared by incubating the coating surfaces with culture medium for different days. As shown in Fig. S7, all the cells were well-grown with spindle, triangular and quadrangular shape. But, the cell viability of L929 cells cultured in the extracts was slightly reduced (82 ~ 86%) after 24-h cultivation as compared with that in the fresh medium. However, no significant decrease could be observed after 48-h

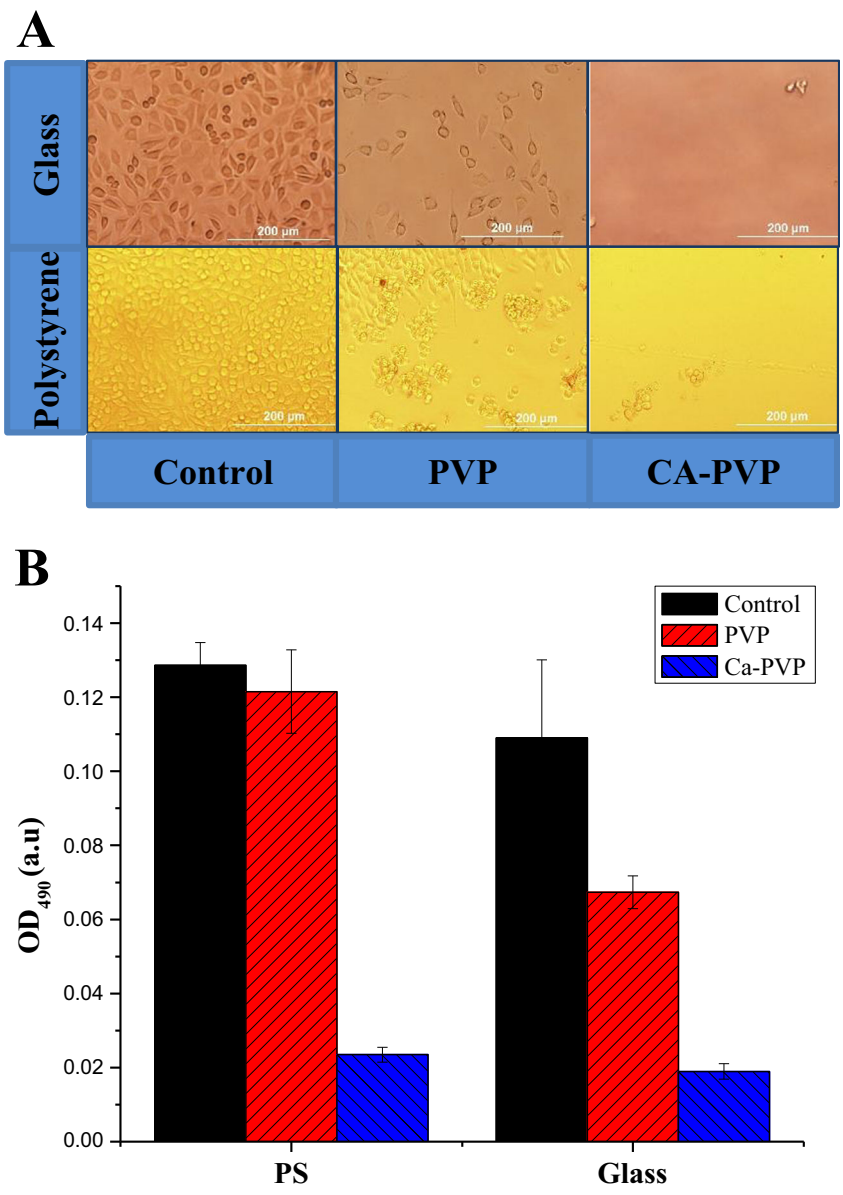

Fig. 7 (**a**) Microscopic images of L929 cell grew on glass and polystyrene substrates (× 10 magnifications) at 37 °C within 24 h and (**b**) OD_{490} of colorimetric LDH assay on cells grew on different coated surfaces

cultivation even when the extraction time was prolonged to 5 days. This clearly indicates that the CA-PVP coating will not cause cytotoxic effect.

Conclusion

Catechol-conjugated PVP (CA-PVP), prepared by reacting PVP with 2-chloro-3, 4′-hydroxyacetophenone, can be well-coated on glass, gold, and TCPS surfaces under a mild condition. Without conjugating with catechol groups, PVP itself did not show much effectiveness on coating onto the glass and TCPS surfaces as demonstrated by their poor performances on changing the surface contact angles and reducing the anti-biofouling ability. But, gold surface can allow PVP itself to be well-adhered and an appreciable protein resistance capability was demonstrated by SPR measurement. In contrast, all the CA-PVP coatings showed much better performance than PVP coatings on protein resistance and anti-biofilm. The CA-PVP-coated surface also showed a strong adhesion resistance against anchorage-dependent mouse fibroblast cells L929. No appreciable cytotoxicity caused by CA-PVP coating could be measured. This new facile biofouling resistant coating may find greater biomedical applications to eliminate the potential infection and adherence problems caused by implanted devices.

Acknowledgements The author Ai-Nhan Au-Duong gratefully acknowledges the scholarship from international graduate program of National Taiwan University of Science and Technology.

Compliance with ethical standards

Conflicts of interest The authors declare that they have no conflict of interest.

References

1. Miquel S, Lagrafeuille R, Souweine B, Forestier C (2016) Anti-biofilm activity as a health issue. Front Microbiol 7:592
2. Lebeaux D, Ghigo JM, Beloin C (2014) Biofilm-related infections: bridging the gap between clinical management and fundamental aspects of recalcitrance toward antibiotics. Microbiol Mol Biol Rev 78(3):510–543
3. Lowe S, O'Brien-Simpson NM, Connal LA (2015) Antibiofouling polymer interfaces: poly(ethylene glycol) and other promising candidates. Polym Chem 6(2):198–212
4. Zhang H, Chiao M (2015) Anti-fouling coatings of poly(dimethylsiloxane) devices for biological and biomedical applications. J Med Biol Eng 35(2):143–155
5. Krishnan S, Weinman CJ, Ober CK (2008) Advances in polymers for anti-biofouling surfaces. J Mater Chem 18(29):3405–3413
6. Zhang M, Cabane E, Claverie J (2007) Transparent antifouling coatings via nanoencapsulation of a biocide. J Appl Polym Sci 105(6):3826–3833
7. Venault A, Huang WY, Hsiao SW, Chinnathambi A, Alharbi SA, Chen H, Zheng J, Chang Y (2016) Zwitterionic modifications for enhancing the antifouling properties of poly(vinylidene fluoride) membranes. Langmuir 32(16):4113–4124
8. Tiller JC, Liao CJ, Lewis K, Klibanov AM (2001) Designing surfaces that kill bacteria on contact. Proc Natl Acad Sci U S A 98(11): 5981–5985
9. Zhu X, Tang L, Wee KH, Zhao YH, Bai R (2011) Immobilization of silver in polypropylene membrane for anti-biofouling performance. Biofouling 27(7):773–786
10. Nurioglu AG, Esteves ACC, de With G (2015) Non-toxic, non-biocide-release antifouling coatings based on molecular structure design for marine applications. J Mater Chem B 3(32):6547–6570
11. Liu X, Tong W, Wu Z, Jiang W (2013) Poly(N-vinylpyrrolidone)-grafted poly(dimethylsiloxane) surfaces with tunable microtopography and anti-biofouling properties. RSC Adv 3(14): 4716–4722
12. Xiang T, Yue WW, Wang R, Liang S, Sun SD, Zhao CS (2013) Surface hydrophilic modification of polyethersulfone membranes by surface-initiated ATRP with enhanced blood compatibility. Colloids Surf B: Biointerfaces 110:15–21
13. Liu X, Xu Y, Wu Z, Chen H (2013) Poly(N-vinylpyrrolidone)-modified surfaces for biomedical applications. Macromol Biosci 13(2):147–154
14. Wu Z, Tong W, Jiang W, Liu X, Wang Y, Chen H (2012) Poly(N-vinylpyrrolidone)-modified poly(dimethylsiloxane) elastomers as anti-biofouling materials. Colloids Surf B: Biointerfaces 96:37–43
15. Yuan H, Qian B, Zhang W, Lan M (2016) Protein adsorption resistance of PVP-modified polyurethane film prepared by surface-initiated atom transfer radical polymerization. Appl Surf Sci 363: 483–489
16. Kuypers MH, GFJ Steeghs, E Brinkman (1990) Method of providing a substrate with a layer comprising a polyvinylbased hydrogel and a biochemically active material. Google Patents
17. Liu Z-M, Xu ZK, Wang JQ, Wu J, Fu JJ (2004) Surface modification of polypropylene microfiltration membranes by graft polymerization of N-vinyl-2-pyrrolidone. Eur Polym J 40(9):2077–2087
18. El-Sawy NM, Elassar AZA (1998) Some modification on radiation graft polymerization of N-vinyl-2-pyrrolidone onto low density polyethylene with α,β-unsaturated nitrile. Eur Polym J 34(8): 1073–1080
19. Liu Z-M, Xu ZK, Wan LS, Wu J, Ulbricht M (2005) Surface modification of polypropylene microfiltration membranes by the immobilization of poly(N-vinyl-2-pyrrolidone): a facile plasma approach. J Membr Sci 249(1–2):21–31
20. Meinhold D, Schweiss R, Zschoche S, Janke A, Baier A, Simon F, Dorschner H, Werner C (2004) Hydrogel characteristics of electron-beam-immobilized poly(vinylpyrrolidone) films on poly(ethylene terephthalate) supports. Langmuir 20(2):396–401
21. Barros JAG, Fechine GJM, Alcantara MR, Catalani LH (2006) Poly(N-vinyl-2-pyrrolidone) hydrogels produced by Fenton reaction. Polymer 47(26):8414–8419
22. Peniche C, Zaldívar D, Pazos M, Páz S, Bulay A, Román JS (1993) Study of the thermal degradation of poly(N-vinyl-2-pyrrolidone) by thermogravimetry–FTIR. J Appl Polym Sci 50(3):485–493
23. Telford AM, James M, Meagher L, Neto C (2010) Thermally cross-linked PNVP films as antifouling coatings for biomedical applications. ACS Appl Mater Interfaces 2(8):2399–2408
24. Lee H, Dellatore SM, Miller WM, Messersmith PB (2007) Mussel-inspired surface chemistry for multifunctional coatings. Science 318(5849):426–430
25. Kang SM, Hwang NS, Yeom J, Park SY, Messersmith PB, Choi IS, Langer R, Anderson DG, Lee H (2012) One-step multipurpose surface functionalization by adhesive catecholamine. Adv Funct Mater 22(14):2949–2955

26. Jiang J, Zhu L, Zhu L, Zhang H, Zhu B, Xu Y (2013) Antifouling and antimicrobial polymer membranes based on bioinspired polydopamine and strong hydrogen-bonded poly(N-vinyl pyrrolidone). ACS Appl Mater Interfaces 5(24):12895–12904
27. Waite JH, Tanzer ML (1981) Polyphenolic substance of *Mytilus edulis*: novel adhesive containing L-Dopa and Hydroxyproline. Science 212(4498):1038–1040
28. Lee Y, Lee H, Kim YB, Kim J, Hyeon T, Park H, Messersmith PB, Park TG (2008) Bioinspired surface immobilization of hyaluronic acid on monodisperse magnetite nanocrystals for targeted cancer imaging. Adv Mater 20(21):4154–4157
29. Neto AI, Meredith HJ, Jenkins CL, Wilker JJ, Mano JF (2013) Combining biomimetic principles from the lotus leaf and mussel adhesive: polystyrene films with superhydrophobic and adhesive layers. RSC Adv 3(24):9352–9356
30. Neto AI, Cibrão AC, Correia CR, Carvalho RR, Luz GM, Ferrer GG, Botelho G, Picart C, Alves NM, Mano JF (2014) Nanostructured polymeric coatings based on chitosan and dopamine-modified hyaluronic acid for biomedical applications. Small 10(12):2459–2469
31. Sun J, Su C, Zhang X, Yin W, Xu J, Yang S (2015) Reversible swelling–shrinking behavior of hydrogen-bonded free-standing thin film stabilized by catechol reaction. Langmuir 31(18):5147–5154
32. Wu J, Zhang L, Wang Y, Long Y, Gao H, Zhang X, Zhao N, Cai Y, Xu J (2011) Mussel-inspired chemistry for robust and surface-modifiable multilayer films. Langmuir 27(22):13684–13691
33. Dalsin JL, Hu BH, Lee BP, Messersmith PB (2003) Mussel adhesive protein mimetic polymers for the preparation of nonfouling surfaces. J Am Chem Soc 125(14):4253–4258
34. Park JY, Yeom J, Kim JS, Lee M, Lee H, Nam YS (2013) Cell-repellant dextran coatings of porous titania using mussel adhesion chemistry. Macromol Biosci 13(11):1511–1519
35. Lee C, Shin J, Lee JS, Byun E, Ryu JH, Um SH, Kim DI, Lee H, Cho SW (2013) Bioinspired, calcium-free alginate hydrogels with tunable physical and mechanical properties and improved biocompatibility. Biomacromolecules 14(6):2004–2013
36. Li A, Mu Y, Jiang W, Wan X (2015) A mussel-inspired adhesive with stronger bonding strength under underwater conditions than under dry conditions. Chem Commun 51(44):9117–9120
37. Mosaiab T, Jeong CJ, Shin GJ, Choi KH, Lee SK, Lee I, in I, Park SY (2013) Recyclable and stable silver deposited magnetic nanoparticles with poly (vinyl pyrrolidone)-catechol coated iron oxide for antimicrobial activity. Mater Sci Eng C 33(7):3786–3794
38. Choi JS, Kim Y, Kang J, Jeong SY, Yoo HS (2013) Electrospun chitosan microspheres for complete encapsulation of anionic proteins: controlling particle size and encapsulation efficiency. AAPS PharmSciTech 14(2):794–801
39. Xiong Y, Washio I, Chen J, Cai H, Li ZY, Xia Y (2006) Poly(vinyl pyrrolidone): a dual functional reductant and stabilizer for the facile synthesis of Noble metal nanoplates in aqueous solutions. Langmuir 22(20):8563–8570
40. Mack D, Becker P, Chatterjee I, Dobinsky S, Knobloch JKM, Peters G, Rohde H, Herrmann M (2004) Mechanisms of biofilm formation in *Staphylococcus epidermidis* and *Staphylococcus aureus*: functional molecules, regulatory circuits, and adaptive responses. Int J Med Microbiol 294(2–3):203–212